The inflammatory cytokine IL-18 induces self-reactive innate antibody responses regulated by natural killer T cells

Sara Lind Enoksson[a], Emilie K. Grasset[a], Thomas Hägglöf[a], Nina Mattsson[a], Ylva Kaiser[a], Susanne Gabrielsson[a], Tracy L. McGaha[b], Annika Scheynius[a], and Mikael C. I. Karlsson[a,1]

[a]Translational Immunology Unit, Department of Medicine Solna, Karolinska Institute, 171 76 Stockholm, Sweden; and [b]Department of Medicine–Section of Nephrology, Immunotherapy Center, Georgia Health Sciences University, Augusta, GA 30912

Edited by Jeffrey V. Ravetch, The Rockefeller University, New York, NY, and approved October 31, 2011 (received for review May 19, 2011)

Inflammatory responses initiate rapid production of IL-1 family cytokines, including IL-18. This cytokine is produced at high levels in inflammatory diseases, including allergy and autoimmunity, and is known to induce IgE production in mice. Here we provide evidence that IL-18 is directly coupled to induction of self-reactive IgM and IgG antibody responses and recruitment of innate B2 B cells residing in the marginal zone of the spleen. Moreover, the data suggest that the B-cell activation occurs predominantly in splenic extrafollicular plasma cell foci and is regulated by natural killer T (NKT) cells that prevent formation of mature germinal centers. We also find evidence that NKT cells control this type of B-cell activation via cytotoxicity mediated by both the perforin and CD95/CD178 pathways. Thus, NKT cells regulate innate antibody responses initiated by an inflammatory stimulus, suggesting a general mechanism that regulates B-cell behavior in inflammation and autoreactivity.

biological sciences | immunology | marginal zone B cells | anti-DNA antibodies

The cytokine IL-18 belongs to the IL-1 family and is, just as IL-1β, activated when cleaved by caspase 1 upon inflammasome activation. Many cell types can produce IL-18, including macrophages, dendritic cells, keratinocytes, and Kupffer cells. IL-18 was initially identified as a factor that enhances IFN-γ production by T helper 1 (Th1) cells together with IL-12; however, IL-18 stimulates a Th2 response when it acts alone or in synergy with IL-2 (1, 2). The Th2 effect of IL-18 includes production of IL-4 and IL-13 (by $CD4^+$ T cells, basophils, and mast cells), up-regulation of CD40L on $CD4^+$ T cells, and production of IgE (3–5). Likewise, overexpression of IL-18 in mice results in chronic inflammation and atopic eczema-like skin lesions (6, 7). Similarly, elevated levels of IL-18 have been reported in patients with atopic eczema (6, 8), as well as in autoimmune diseases such as rheumatoid arthritis, systemic lupus erythematosus, and Sjögren's syndrome (9), suggesting a link between IL-18 and multiple chronic inflammatory diseases.

The IL-18 receptor (IL-18R) is part of the IL-1R/TLR superfamily signaling via a MyD88-dependent pathway. A wide range of cells including T cells, natural killer (NK) cells, natural killer T (NKT) cells, mast cells, and basophils express the IL-18R (2). Accordingly, IL-18–induced antibody production in mice has been shown to be dependent on IL-4–producing $CD4^+$ T cells (3, 5, 10). Nevertheless, although the T-cell response in IL-18–induced antibody production has been thoroughly investigated, it is still not understood mechanistically how the B-cell activation occurs and which B-cell population(s) are involved in the response. Likewise, the nature and function of the antibody response also remain to be investigated.

The mature naive B-cell repertoire consists of B1 and B2 B cells, and the latter includes the follicular B-cell (FoB) and the marginal zone B-cell (MZB) subtypes. FoBs are recirculating cells that preferentially participate in classical adaptive T-cell–dependent antibody responses to protein antigens whereas MZBs and B1 B cells are more innate-like resident B cells located in the marginal zone of the spleen and peritoneal cavity, respectively (11, 12). MZBs and B1 B cells are an important source of innate antibodies as their B-cell receptor (BCR) repertoire includes germ-line encoded BCRs with limited diversity that recognize conserved structures common to both self and bacterial antigens (13). Innate, or natural, antibodies are sometimes referred to as polyreactive in that they bind structurally unrelated antigens such as insulin and dsDNA (14). In connection to innate B-cell activation, MZBs express high levels of CD1d (12) whereby they can interact with the innate-like T-cell subset called NKT cells (15).

NKT cells serve as a functional bridge between the innate and adaptive immune response and the majority expresses a semi-invariant T-cell receptor (TCR), invariant α-chain Vα14-Jα18 paired with Vβ8.2/Vβ7/Vβ2, which recognizes glycolipid antigens presented on the MHC class I-like molecule CD1d. These antigens include both endogenous and exogenous glycolipids and activation via the TCR leads to rapid induction of effector functions such as cytotoxicity and release of large amounts of IFN-γ and IL-4 with potent immune regulatory functions (12, 16). Consequently, NKT cells have been implicated in the regulation of a variety of immune responses. Studies in mouse models and patients with autoimmune disease have shown that a reduction in NKT cells often is associated with a more severe disease (17). In line with this, we have previously reported that NKT cells limit autoimmunity induced by injections of apoptotic cells (18).

In this report, we investigated the innate B-cell response in IL-18–mediated inflammation and found that IL-18 induced production of self-reactive IgM and IgG antibodies with innate reactivities as well as a potent IgE response. The B-cell activation was primarily confined to plasma cell foci and included recruitment of MZBs and increased production of the cytokine B-cell activating factor of the TNF family (BAFF). Moreover, NKT cells regulated the IL-18–induced antibody response by preventing the formation of mature germinal centers (GCs). Thus, we have uncovered a mechanism coupling inflammation to activation of MZBs and innate antibody production controlled by NKT cells.

Results

IL-18 Injections Give Rise to Production of Innate Antibodies. Increased levels of IL-18 have been connected to several diseases where antibodies play an important role in the pathology (6, 8, 9) and we therefore analyzed the serum levels of IgM, IgG, and IgE in IL-18–injected mice (Fig. 1*A*). In line with previous studies (3, 5),

Author contributions: S.L.E., E.K.G., S.G., T.L.M., and M.C.I.K. designed research; S.L.E., E.K.G., T.H., Y.K., N.M., and M.C.I.K. performed research; S.L.E., E.K.G., T.H., and M.C.I.K. analyzed data; and S.L.E., A.S., and M.C.I.K. wrote the paper.

The authors declare no conflict of interest.

This article is a PNAS Direct Submission.

[1]To whom correspondence should be addressed. E-mail: mikael.karlsson@ki.se.

See Author Summary on page 20285.

This article contains supporting information online at www.pnas.org/lookup/suppl/doi:10.1073/pnas.1107830108/-/DCSupplemental.

injections of IL-18 resulted in increased serum levels of IgE after 10 d compared with those in PBS-injected mice (Fig. S1). Interestingly, we also observed increased serum levels of total IgM and IgG after 10–12 d in IL-18–injected mice (Fig. 1*B*). Analysis of the different subclasses of IgG revealed an increase in IgG_1 and IgG_{2a}, and to a lesser extent in IgG_{2b}, whereas IgG_3 remained unchanged (Fig. 1*C*). The fact that IL-18 signals through MyD88 and gives rise to IgG and IgE production indicates that this cytokine is involved in an innate-type activation of the immune system that subsequently results in an early isotype-switched antibody response. Therefore, we analyzed serum of IL-18–injected mice for antibodies derived from the inherited polyreactive repertoire and found increased levels of both IgM and IgG specific for phosphorylcholine (PC), DNA, and 4-hydroxy-3-nitrophenyl (NP) (Fig. 1*D*).

The most striking change observed when analyzing the serum antibody levels in IL-18–injected mice was the 20-fold increase in total-IgE levels. We therefore used an in vitro culture system with bone marrow-derived mast cells (BMMCs) to evaluate the significance of this IgE response for subsequent inflammatory events. BMMCs were loaded with sera from untreated or IL-18–injected mice followed by anti-IgE cross-linking and analysis of degranulation. The sera from IL-18–injected mice induced a marked degranulation of the BMMCs, measured by β-hexosaminidase release, whereas the sera from untreated mice had no detectable effect (Fig. 1*E*). Thus, the serum IgE response induced by IL-18 is sufficient to prime an inflammatory mast cell response.

Antibody Production and MZB Expansion in the Spleens of IL-18–Injected Mice. After finding that IL-18 increases the production of autoreactive antibodies, we wanted to investigate where IL-18–mediated B-cell activation takes place and which B-cell subset(s) are involved. The innate-like B cells that produce these antibodies are known to be located in the spleen (MZBs) and peritoneum (B1a cells). Splenocytes and peritoneal cells from IL-18–injected mice were thus cultured ex vivo followed by measurement of antibodies in the culture supernatants. Production of total IgE, IgG, and IgM increased in the splenocyte cultures, whereas IL-18 injections had no impact on the antibody production by peritoneal cells (Fig. 2*A*). Further analysis of the spleen as a target organ for IL-18–induced antibody production showed that the IL-18R is expressed by cells in the splenic T-cell zone and red pulp area (Fig. S2*A*). Costaining for CD4 and F4/80 confirmed that the IL-18R–expressing cells were T cells and macrophages, respectively. The $CD4^+$ IL-18R–expressing cells included both T cells and NKT cells, demonstrated by flow cytometry (Fig. S2*B*).

Mature splenic B cells express very low levels, if any, of the IL-18R (19) (Fig. S2*C*). Nevertheless, analysis of the FoBs, MZBs, and B1a cells in the spleens of IL-18–injected mice showed that the MZB population expanded significantly after 6 d of IL-18 injections, whereas the FoB and B1a populations remained unchanged (Fig. 2*B* and Fig. S3*A*). The enlargement of the MZB compartment was confirmed by an increase in absolute MZB numbers (Fig. 2*B*, *Right*) as well as by histological analysis showing an expansion of the $CD1d^{hi}$ cells in the marginal zone of the spleen (Fig. 2*C*). The increased MZB population could be due to either expansion of existing MZBs or development from immature transitional B cells. Analysis of the transitional B-cell subsets after 6 d of IL-18 injections showed a decrease in the transitional type 1 (T1) and type 2 (T2) B cells and no difference in the T2-MZ precursor (T2-MZP) subset (Fig. S3*B*). These results indicate that IL-18 drives expansion of MZBs, possibly by stimulating differentiation from transitional precursors.

IL-18–induced antibody responses have been shown to involve switching to Th2-type cytokines (especially IL-4) and to be dependent on $CD4^+$ T cells (3, 5). To investigate whether the expansion of MZB is driven by $CD4^+$ T-cell–dependent signals, we analyzed the MZB population after 6 d of IL-18 injections in WT (C57BL/6) and $CD4^{-/-}$ (20) mice (Fig. 2*D*). The MZB pop-

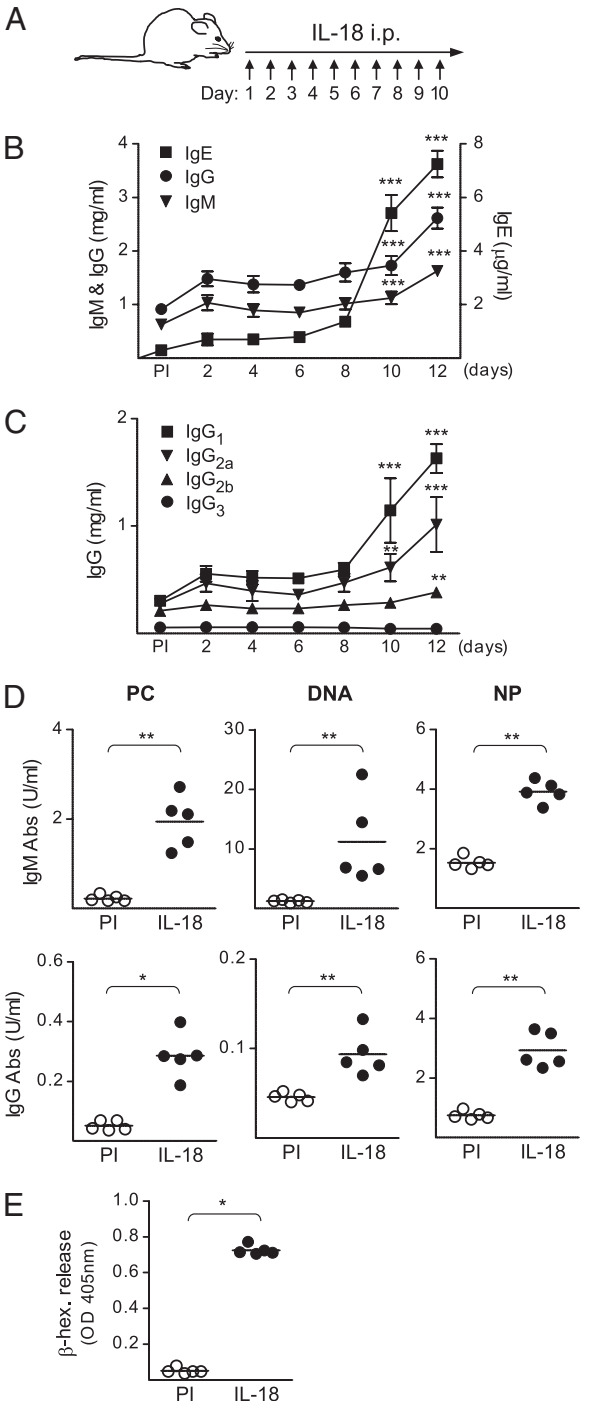

Fig. 1. The levels of total IgM, IgG, and IgE as well as innate antibodies increase in serum of IL-18–injected mice. (*A*) Schematic outline of the IL-18 injections in WT (129/SvEv) mice. (*B* and *C*) Serum levels of (*B*) total IgM, IgG, and IgE and (*C*) total IgG_1, IgG_{2a}, IgG_{2b}, and IgG_3 in IL-18–injected mice. Mean and SEM from 5 to 25 mice per group [preimmune (PI) and indicated time points] are plotted. (*D*) Serum levels of IgM and IgG reactive with PC, DNA, and NP in IL-18–injected mice. Mean and individual mice (PI and day 12) are plotted. (*E*) The increased IgE levels in IL-18–injected mice induce mast cell degranulation. β-Hexosaminidase (β-hex) released from BMMCs incubated with sera from untreated or IL-18–injected mice, followed by anti-IgE cross-linking. Mean and individual mice (PI and day 12) are plotted. $*P < 0.05$, $**P < 0.01$, and $***P < 0.001$ by comparing IL-18–injected mice to the PI group with a Mann–Whitney test.

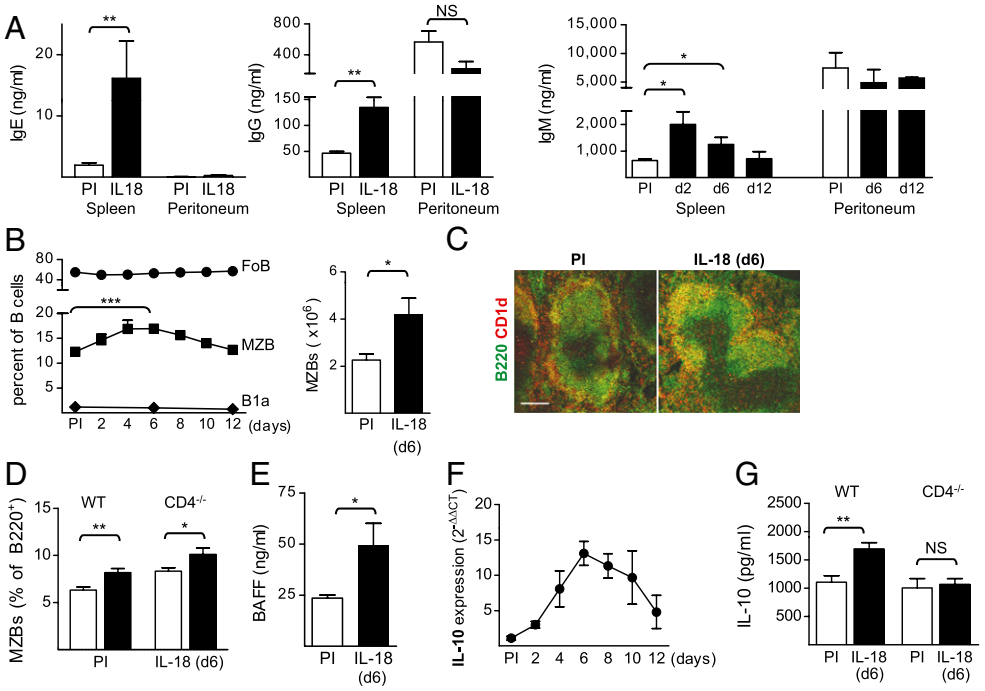

Fig. 2. IL-18 injections induce antibody production and MZB expansion in the spleen. (*A*) Total IgE, IgG, and IgM produced in ex vivo splenocyte and peritoneal cell cultures from IL-18–injected mice. Mean and SEM from 3 to 10 mice per group [pre immune (PI) and day 12 or indicated time points] are plotted. (*B–D*) Analysis of the B-cell subsets in the spleen of IL-18–injected mice. (*B*) FACS analysis of FoBs, MZBs, and B1a cells (*Left*) and absolute MZB numbers (*Right*). Mean and SEM from 3 to 10 mice per group are plotted. (*C*) Immunofluorescence of the spleen for CD1d^{hi} MZBs (orange) in untreated (PI) and IL-18–injected mice (day 6). (Scale bar, 150 μm.) (*D*) FACS analysis of MZBs in WT (C57BL/6) and CD4$^{-/-}$ mice. Mean and SEM from 5 to 6 mice per group (PI and day 6) are plotted. (*E*) Serum level of BAFF in IL-18–injected mice. Mean and SEM from 3 to 5 mice per group (PI and day 10) are plotted. (*F*) Expression of mRNA for *il10* in the spleen of IL-18–injected mice measured with quantitative PCR. Mean and SEM (PI and indicated time points) are plotted. Relative expression was normalized to that of *gapdh* and the Δ*Ct* values from IL-18–injected mice were compared with the mean Δ*Ct* value of the PI mice. (*G*) IL-10 produced in LPS stimulated ex vivo splenocyte cultures from IL-18–injected WT and CD4$^{-/-}$ mice. Mean and SEM from 5 to 6 mice per group (PI and day 6) are plotted. **P* < 0.05, ***P* < 0.01, and ****P* < 0.001 by comparing IL-18–injected mice to the PI group with a Mann–Whitney test.

ulation expanded in both WT and CD4$^{-/-}$ mice, indicating that the IL-18–induced MZB expansion is independent of CD4^{+} T cells. Another candidate for driving the MZB expansion is the TNF-family member BAFF, which is known to be important for survival and activation of MZBs (21). In line with this, we found increased levels of BAFF in the serum of IL-18–injected mice (Fig. 2*E*).

Regulatory B cells are a CD1d^{hi} population that is thought to be enriched within the T2-MZP population (22). To investigate whether there is an expansion of regulatory B cells in the spleen of IL-18–injected mice, we analyzed expression of IL-10 and found it to be increased with the peak at day 6 of the response (Fig. 2*F*). To define whether the increase in IL-10 is a product of regulatory B and/or T cells, we investigated the IL-10 response in WT and CD4$^{-/-}$ mice. The mice were first injected with IL-18 for 6 d and the splenocytes were thereafter stimulated with LPS in vitro followed by measurement of IL-10 in the culture supernatant. There was neglectable production of IL-10 in cultures that did not receive LPS stimulation, regardless of genotype or in vivo treatment (<15 pg/mL). In the LPS-stimulated cultures, IL-18 injections augmented the IL-10 production from WT, but not CD4$^{-/-}$, mice (Fig. 2*G*), indicating that the increased expression of IL-10 mRNA in the spleen of IL-18–injected mice is not a B-cell–intrinsic effect but rather dependent on CD4^{+} T cells. In summary, IL-18 recruits B-cell precursors into the MZB pool by inducing production of BAFF, independent of T-cell–derived signals. However, IL-10 production is dependent on T cells whereas IL-18 does not recruit regulatory B cells.

Delayed Early Antibody Response in MZB-Deficient Mice Injected with IL-18. The production of innate antibodies along with B-cell activation and MZB expansion in the spleen in IL-18–injected mice suggested that the MZB subset is highly involved in the IL-18–mediated antibody response. We thus injected CD19$^{-/-}$ mice, which are deficient in MZBs but have an intact FoB population (23), with IL-18 to assess the contribution of MZBs to this early antibody response. Unexpectedly, a B-cell population with MZB phenotype (CD21^{hi}/CD23^{-}) was allowed to develop in CD19$^{-/-}$ mice after IL-18 injections (Fig. 3*A* and Fig. S4*A*). The MZB phenotype was confirmed by histological examination, which showed that this new B-cell population was CD1d^{hi} and located in the marginal zone of the spleen (Fig. 3*A*). Compared with the WT controls (129/SvEv), the antibody levels were lower in the CD19$^{-/-}$ mice in the early phase of the response (day 6) but reached the same level as in the WT mice after 10 d of IL-18 injections (Fig. 3*B*). Taken together, these results suggest that IL-18 can overcome the MZB developmental defect in CD19$^{-/-}$ mice and that this B-cell subset may contribute to the antibody response induced by IL-18 when the population is sufficiently expanded.

As shown in Fig. 2*E*, the serum levels of BAFF increase after IL-18 injections in WT mice and we found the serum levels of BAFF to be elevated also in IL-18–injected CD19$^{-/-}$ mice (Fig. 3*C*). BAFF is thus likely to drive the development of MZBs in CD19$^{-/-}$ mice after IL-18 injections. In line with this, we found that injections of recombinant BAFF were able to induce development of MZBs in CD19$^{-/-}$ mice (Fig. 3*D* and Fig. S4*B*).

B-Cell Activation in Extrafollicular Foci and Immature GCs in the Spleens of IL-18–Injected Mice. Activated B cells can differentiate either to antibody-producing cells in follicles, where they form GCs, or in foci in extrafollicular sites (24). In the spleen, MZBs

have been suggested to preferably and more rapidly be recruited to extrafollicular antibody responses compared with FoBs (24, 25). Histological examination of the spleen of IL-18–injected mice revealed formation of both GCs and extrafollicular foci (Fig. 4*A*). IgE and IgG_1 antibodies dominate the switched antibody response in IL-18–injected mice and both IgE- and IgG_1-expressing B cells were detected at extrafollicular sites (Fig. 4*B*). The IgE^+ and $IgG_1{}^+$ foci were located either in proximity to the marginal zone or at the T-cell zone/red pulp boarder.

B cells in GCs can be distinguished from plasma cells in extrafollicular foci by differential expression of the BCR and the CD45 isoform B220; GC B cells are $B220^+/BCR^+$ whereas plasma cells are $B220^{low}/BCR^{hi}$ (26). The IgG_1-expressing B cells in IL-18–injected mice were of either plasma cell ($B220^{low}/IgG_1{}^{hi}$) or GC ($B220^+/IgG_1{}^+$) phenotype, whereas the majority of the IgE-expressing B cells were $B220^{low}/IgE^{hi}$ plasma cells (Fig. 4 *C* and *D*). The BCR^{hi} cells were also $CD138^+$ (Fig. 4 *C* and *D*), thus confirming a plasma cell phenotype (27). Both IgE- and IgG_1-expressing B cells appeared in extrafollicular foci at day 10 of IL-18 injections whereas GCs were not formed until day 12 (Fig. 4*E*). These results suggest that the B-cell activation via IL-18 takes place in extrafollicular foci followed by GC formation.

Several genes are differentially regulated when B cells are activated to enter GCs or extrafollicular foci. Of these, activation-induced deaminase (*aid*) is up-regulated in GC B cells (28) whereas Epstein–Barr virus-induced gene 2 (*ebi2*) is down-regulated in GC B cells and up-regulated in extrafollicular foci (29–31). In the spleen of IL-18–injected mice, the expression of *ebi2* mRNA was up-regulated at day 6 followed by a down-regulation at day 12, consistent with extrafollicular foci and GC formation, respectively (Fig. 4*F*). However, although we identified GCs with both histology and flow cytometry, we could not detect up-regulation of *aid* mRNA in the spleen of IL-18–injected mice (Fig. 4*G*). These results suggest formation of either underdeveloped GCs or innate-type GCs similar to the T-cell–independent GCs that have been reported to be induced by immune complexes (32). Taken together, our results demonstrate that injections of IL-18 expand the MZB compartment and lead to isotype switch and production of innate-type antibodies in extrafollicular foci and immature GCs.

NKT Cells Control the Antibody Response in Mice Injected with IL-18. We recently showed that B-cell entry into GCs can be regulated by NKT cells (18) and alterations in the NKT cell population as well as increased levels of IL-18 have been reported in several inflammatory diseases (8, 9, 17). These findings together with our present data that IL-18 induces production of innate antibodies (which are enriched within the $CD1d^{hi}$ MZB subset) (13) prompted us to test whether NKT cells regulate B-cell activation by this inflammatory cytokine. The IL-18–induced antibody response was investigated in two different NKT cell-deficient mouse strains, $CD1d^{-/-}$ and $J\alpha18^{-/-}$ (where Jα18 is the α-chain of the TCR used by invariant NKT cells), as well as in WT (C57BL/6) control mice. In the absence of NKT cells, the isotype-switched antibody response was significantly increased (Fig. 5*A*), suggesting that activated NKT cells negatively regulate this type of B-cell activation.

The data described above are in opposition to a previous study using CD1d-deficient mice, which suggested that the absence of NKT cells attenuates the IgE response to IL-18 (10). However, this study used a different, independently generated, CD1d-deficient mouse strain ($CD1d1^{-/-}$ mice) (33). To investigate these seemingly disparate results, we investigated the IL-18–induced IgE response in this CD1d-deficient strain. In accordance with the previously published observation, we found that injection of the alternate CD1d-deficient mouse strain with IL-18 induced an IgE response that was lower compared with that in WT (C57BL/6) mice (Fig. S5*A*). Surprisingly, when splenic lymphocyte populations were examined, we found a specific deficiency in the MZB subset in the alternate CD1d-deficient mice (Fig. S5*B*). There were no differences in other populations examined (T cells, monocytes, dendritic cells, and neutrophils) or in expression of the IL-18R in the spleen of the $CD1d1^{-/-}$ mice. The MZB deficiency was observed in mice that were backcrossed 6 generations, whereas $CD1d1^{-/-}$ mice backcrossed 12 generations had a normal MZB population (Fig. S5*C*). The concurrence of MZB deficiency and reduced IgE response to IL-18 supports a role for MZBs in IL-18–induced antibody production. In line with this result, bone marrow (BM) transfer from $CD1d^{-/-}$ mice to $CD1d1^{-/-}$ mice restored both the IL-18–induced IgE response and the MZB population (Fig. S5 *D* and *E*).

IgE levels in serum are normally low, but have been reported to increase in WT mice with age (34). To investigate whether absence of NKT cells also affects long-term accumulation of IgE antibodies, we measured serum levels of IgE in NKT cell-deficient and WT mice over time. We found the IgE levels in NKT cell-deficient mice to be approximately four times those of WT mice at 8 mo of age (Fig. 5*B*). Taken together, these results indicate that NKT cells regulate antibody responses induced by the inflammatory cytokine IL-18 as well as natural IgE levels.

To further investigate how, and at what stage, NKT cells regulate the IL-18–induced antibody response, we compared the formation of extrafollicular foci and GCs after IL-18 injections in WT and NKT cell-deficient mice. Histological analysis of the spleen showed that absence of NKT cells resulted in higher prevalence of both extrafollicular foci (Fig. 5*C*) and GCs (Fig. 5*D*) in IL-18–injected mice. The increased GC formation was further supported by down-regulation of *ebi2* and up-regulation

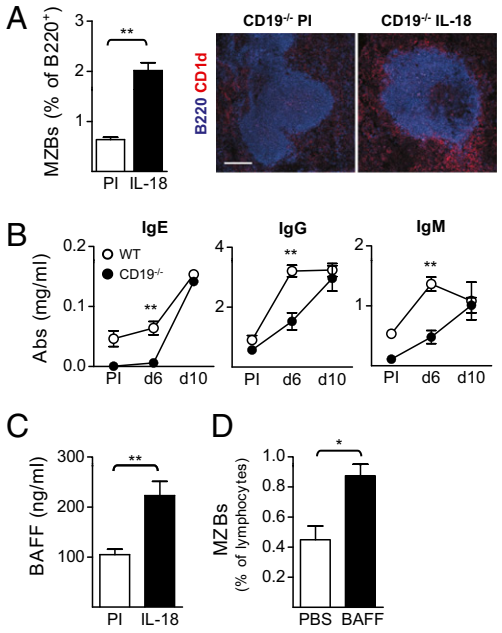

Fig. 3. Development of an MZB population and delayed antibody response in $CD19^{-/-}$ mice injected with IL-18. (*A*) Analysis of the MZBs in the spleen of $CD19^{-/-}$ mice injected with IL-18 [pre immune (PI) and day 10]. FACS data are shown as mean and SEM from six mice per group and the immunofluorescence shows $CD1d^{hi}$ MZBs (red) outside of the follicle (blue). (Scale bar, 150 μm.) (*B*) Serum levels of total IgE, IgG, and IgM in $CD19^{-/-}$ and WT mice injected with IL-18. Mean and SEM from five mice per group (PI and indicated time points) are plotted. (*C*) Serum levels of BAFF in $CD19^{-/-}$ mice injected with IL-18. Mean and SEM from six mice per group (PI and day 10) are plotted. (*D*) FACS analysis of MZBs in $CD19^{-/-}$ mice injected with BAFF. Mean and SEM from three mice per group are plotted. $*P < 0.05$ and $**P < 0.01$ by comparing injected mice to the control group (*A*, *C*, and *D*) or $CD19^{-/-}$ mice to the WT group (*B*) with a Mann–Whitney test.

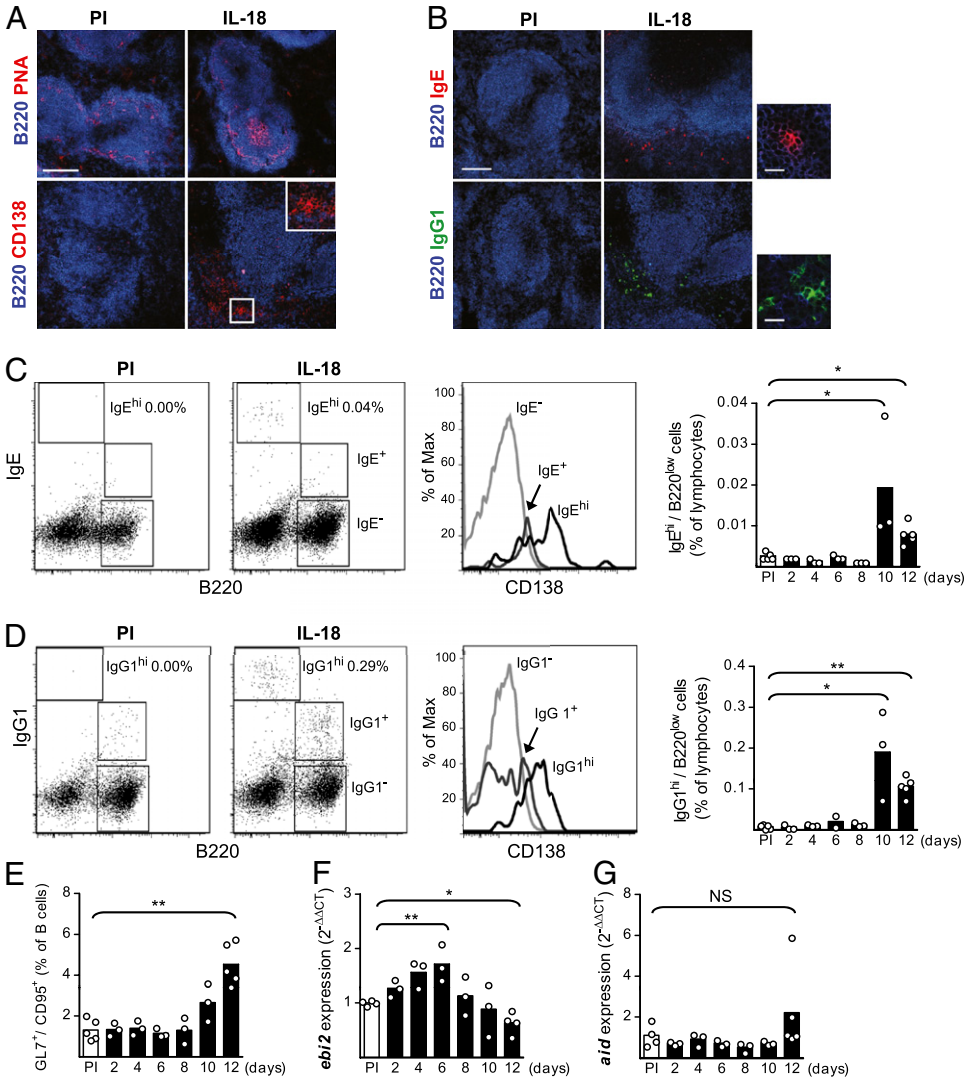

Fig. 4. Activated B cells form extrafollicular foci and immature GCs in the spleen of IL-18–injected mice. (*A*) Immunofluorescence of the spleen for PNA$^+$ GCs (pink), day 12 (*Upper*), and CD138$^+$ extrafollicular foci (red), day 10 (*Lower*), in IL-18–injected mice (PI, preimmune). *Inset* shows the boxed area in higher magnification. (*B*) Immunofluorescence of the spleen for IgE$^+$ (red) and IgG1$^+$ (green) plasma cell foci in IL-18–injected mice, day 10. (Scale bar, 150 μm.) (*Right*) IgE/IgG1 positive foci in higher magnification. (Scale bar, 20 μm.) (*C* and *D*) FACS analysis of isotype-switched B cells with extrafollicular foci (BCR^{hi}/B220^{low}) or GC (BCR^{low}/B220$^+$) phenotype in IL-18–injected mice. Mean and individual mice (PI and indicated time points) as well as representative FACS plots of the gating on splenic lymphocytes (PI and day 10) and expression of CD138 are shown. (*E*) FACS analysis of GCs in the spleen of IL-18–injected mice. Mean and individual mice (PI and indicated time points) are plotted. (*F* and *G*) Expression of mRNA for (*F*) *ebi2* and (*G*) *aid* in the spleen of IL-18–injected mice measured with quantitative PCR. Mean and individual mice (PI and indicated time points) are plotted. Relative expression of *ebi2* and *aid* was normalized to that of *gapdh* and the Δ*Ct* values from IL-18–injected mice were compared with the mean Δ*Ct* value of the PI mice. *$P < 0.05$ and **$P < 0.01$ by comparing IL-18–injected mice to the PI group with a Mann–Whitney test.

of *aid* in NKT cell-deficient mice, whereas the expression of these genes remained unchanged in WT controls after IL-18 injections (Fig. 5*E*). There is thus an increased rate of plasma cell differentiation as well as a shift toward a mature GC phenotype in the absence of NKT cells.

To evaluate how the shift toward a more mature GC phenotype affected the affinity of the antibodies induced by IL-18, we analyzed the NP reactivity in sera from IL-18–injected mice. We found that the IgM and IgG response to high-coupled NP_{26}-BSA was increased in the absence of NKT cells (Fig. 5*F*), as measured by ELISA. Subsequently, using a sensitive quartz crystal microbalance detector, we found that only serum from IL-18–injected NKT cell-deficient mice could bind to low-coupled immobilized NP_4-BSA (Fig. 5*G*). This result shows that in the absence of NKT cells, B cells are allowed to produce high-affinity antibodies. Taken together, our results show that NKT cells balance the IL-18–induced B-cell activation and provide a checkpoint where B cells that produce self-reactive antibodies are prevented from entering GCs.

NKT Cells Regulate IL-18–Induced Antibody Responses Through Cytotoxicity. Next, we sought to investigate the effector mechanism(s) NKT cells use to inhibit the IL-18–induced antibody response. Injection of IL-18 in combination with the potent NKT cell-activating ligand α-galactosylceramide (αGalCer) resulted in a significantly decreased IgE response (Fig. 6*A*). Upon activation, NKT cells rapidly produce large amounts of Th1- and Th2-type cytokines (12) and we observed a tendency toward a transient increase in expression of both IFN-γ and IL-4 on days 4–8 in the spleens of IL-18–injected mice (Fig. S6 *A* and *B*). Production of IL-4 by CD4$^+$ T cells has been reported to be essential for IL-18–induced antibody responses (3, 5) but the role

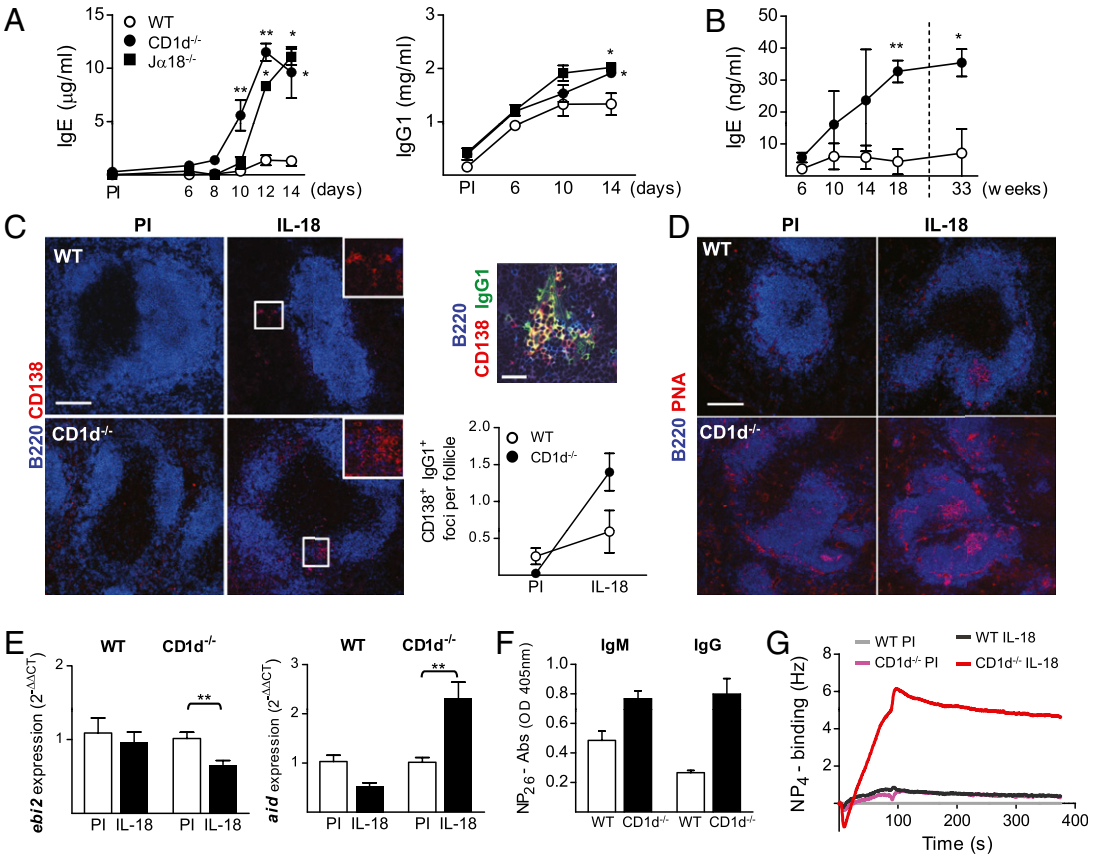

Fig. 5. Increased antibody production, GC formation, and affinity for NP in the absence of NKT cells. (*A*) Serum levels of total IgE and IgG_1 in NKT cell-deficient ($CD1d^{-/-}$ and $J\alpha18^{-/-}$) and WT (C57BL/6) mice injected with IL-18. Mean and SEM from four to five mice per group [preimmune (PI) and indicated time points] are plotted. (*B*) Serum levels of total IgE in untreated $CD1d^{-/-}$ and WT mice over time. Mean and SEM from three to four mice per group are plotted. (*C*) Immunofluorescence of the spleen for $CD138^+$ extrafollicular plasma cells (red) in $CD1d^{-/-}$ and WT mice injected with IL-18 (PI and day 14). (Scale bar, 150 μm.) *Inset* shows boxed area in higher magnification. Plot shows quantification of the plasma cell foci by a blinded observer and mean and SEM from three to four mice per group (PI and day 14). The foci were defined as $B220^{low}$ $CD138^+$ $IgG1^+$ clusters (yellow), illustrated here by foci from an IL-18–injected $CD1d^{-/-}$ mouse. (Scale bar, 30 μm.) (*D*) Immunofluorescence of the spleen for PNA^+ GCs (pink) in $CD1d^{-/-}$ and WT mice injected with IL-18 (PI and day 14). (Scale bar, 150 μm.) (*E*) Expression of mRNA for *ebi2* and *aid* in the spleen of IL-18–injected $CD1d^{-/-}$ and WT mice measured with quantitative PCR. Mean and SEM from five mice per group (PI and day 14) are plotted. Relative expression of transcript was normalized to that of *gapdh* and the Δ*Ct* values from IL-18–injected mice were compared with the mean Δ*Ct* value of the PI mice. (*F* and *G*) Measurement of the high-affinity anti-NP response in sera from IL-18–injected $CD1d^{-/-}$ and WT mice. (*F*) Total IgM and IgG anti-NP antibodies binding to NP_{26}-BSA, measured by ELISA. Mean and SEM from three to five mice per group (PI and day 14) are plotted. (*G*) Presence of high-affinity anti-NP antibodies determined by binding of pooled sera from the indicated groups to NP_4-BSA immobilized on a carboxyl-chip. Binding was detected as changes in frequency measured using an Attana 100; the background signal from nonbinding sera has been subtracted. $*P < 0.05$ and $**P < 0.01$ by comparing knockout mice to the WT group (*A* and *B*) or IL-18–injected mice to the PI group (*E*) with a Mann–Whitney test.

of IFN-γ has yet to be thoroughly investigated in this model. We found that splenic T cells from IL-18–injected mice had a decreased capacity to produce IFN-γ upon in vitro restimulation (Fig. S6*C*). This result is in line with our previous observation that NKT cells limit activation of autoreactive B cells by shifting toward a less proinflammatory cytokine profile (18). However, lack of IFNγR activity (35) had no impact on the serum levels of IgE after IL-18 injections (Fig. S5*D*). Thus, activation of NKT cells inhibits IL-18–induced antibody production, but the mechanism does not involve regulation of the balance between Th1- and Th2-type cytokines.

It has recently been shown that NKT cells are a major source of IL-21 and this cytokine also activates NKT cells and enhances their cytotoxicity (36). Interestingly, IL-21 has also been shown to inhibit IgE production (37). When investigating cytokine production induced by IL-18, we found the expression of IL-21 to be increased in the spleen (Fig. 6*B*). IL-21 could thus be a plausible effector mechanism by which NKT cells regulate this type of B-cell response. NKT cell-mediated killing of B cells in vivo has been shown to directly correlate with the expression level of CD1d (16). The cytotoxic ability of NKT cells includes release of perforin and up-regulation of CD178 (FasL) (38). When testing involvement of cytotoxicity, we found the IL-18–induced antibody response to be increased in mice that lack either perforin or CD178 (Fig. 6 *C* and *D*). These results show that cytotoxicity is an important mechanism in regulation of IL-18–induced antibody production. The cytotoxic effects could be mediated by other cells than NKT cells, such as NK cells and $CD8^+$ T cells. However, it has been shown that absence of NK cells or $CD8^+$ T cells has no impact on IL-18–induced antibody responses (3). It is therefore likely that the observed phenotype in the perforin- and CD178-deficient mice is due to decreased NKT cell cytotoxicity that allows B cells to survive and enter GCs.

Discussion

Production of bioactive IL-18 results from activation of the inflammasome, which plays an important role in both autoinflammatory and adaptive immune responses (2). As an example, the adjuvant alum induces production of IL-1β and IL-18 by

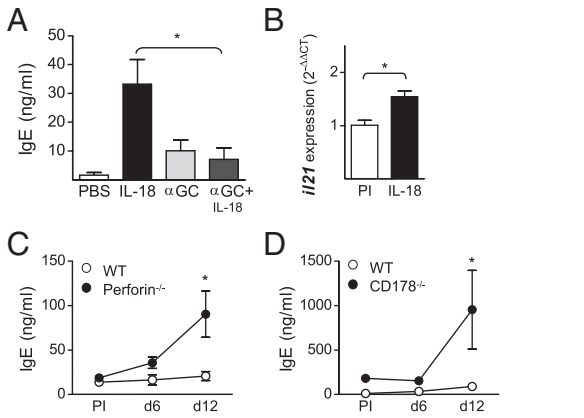

Fig. 6. Increased IL-18–induced antibody response in mice with impaired cytotoxicity. (*A*) Serum levels of total IgE in WT mice injected with IL-18 or PBS in combination with αGalCer (αGC). Mean and SEM from five mice per group at day 12 are plotted. (*B*) Expression of mRNA for *il21* in the spleen of IL-18–injected WT mice measured with quantitative PCR. Mean and individual mice [preimmune (PI) and day 12] are plotted. Relative expression of *il21* was normalized to that of *gapdh* and the ΔCt values from IL-18–injected mice were compared with the mean ΔCt value of the PI mice. (*C* and *D*) Serum levels of total IgE in IL-18–injected mice deficient in perforin (*C*) or CD178/FasL (*D*). Mean and SEM from four to six mice per group (PI and indicated time points) are plotted. *$P < 0.05$ by comparing αGalCer treated to IL-18 alone (*A*), IL-18 injected to controls (*B*), or knockout mice to WT (*C* and *D*) with a Mann–Whitney test.

the NALP3 inflammasome, and this process is crucial for its immunostimulatory properties (39, 40). In the transition to adaptive immunity, $CD4^+$ T-cell–derived IL-4 has been shown to be essential for IL-18–induced antibody responses (3, 5, 10). We have now investigated the B-cell biology behind IL-18–induced antibody production and find that NKT cells are important regulators of this self-reactive humoral response.

Our results show that IL-18–induced antibody production involves activation of an inducible innate antibody response that includes self-reactive reactivities, such as DNA and PC, as well as NP, which are known to be enriched in the naive repertoire (14, 41). Furthermore, the IL-18–induced B-cell response involves activation and expansion of the innate-type MZB subset and subsequent production of antibodies in the spleen by formation of extrafollicular foci and immature GCs. We also find that NKT cells limit this self-reactive B-cell response by regulating the extent of GC formation and plasma cell foci accumulation. Previous studies of IL-18–induced antibody production have mainly focused on the increased levels of IgE antibodies (3, 5, 10). Our detailed investigation of the antibody response in serum shows an increase also in the total levels of IgM and IgG and that the IgG response mainly is of the IgG_1 subclass, consistent with the increased total-IgG_1 levels in caspase-1 transgenic (Tg) mice (5). Thus, we now directly link elevated levels of IL-18 to production of potentially pathogenic isotype-switched self-reactive antibodies, which is in line with the elevated levels of this cytokine in autoimmune conditions (9).

Antibodies produced in extrafollicular foci are composed almost exclusively of specificities found within the primary repertoire (42). An important component in the choice between GC and extrafollicular foci is the BCR–antigen affinity, and only B cells with sufficiently high affinity for the antigen can enter the extrafollicular pathway (43). Regulation of the extrafollicular foci response is also mediated by cytokines, and especially BAFF, which we find to be elevated in IL-18–injected mice, has been suggested to be an important factor (44). Moreover, BAFF Tg mice develop autoimmune manifestations (21) and increased serum levels of BAFF have been reported in a number of autoimmune and allergic conditions (45, 46). In relation to autoimmune disease, mounting evidence now shows that expansion of autoreactive B cells can take place at extrafollicular sites (44, 47). However, the GC is essential for the generation of high-affinity truly pathogenic autoantibodies (42). These findings are consistent with our observation that the B-cell activation in IL-18–driven production of self-reactive antibodies occurs in extrafollicular foci and GC-like structures. However, the IgE-switched B cells were almost solely confined to extrafollicular foci, indicating that these B cells are regulated differently from the IgG_1-expressing cells. This result suggests that different regulatory mechanisms may apply to different subclasses and that particularly IgE is excluded from reactions associated with affinity maturation. Of importance is the low-level expression of *aid*, which suggests that the GCs are not fully mature. Thus, this pattern of B-cell activation mimics that of T-cell–independent antigens, suggesting similarities in the responses (48).

NKT cells have been ascribed both initiating and inhibitory actions in various mouse models for human disease (17). In the IL-18–induced innate antibody response, we find that NKT cells dampen B-cell activation, as illustrated by increased antibody production in NKT cell-deficient mice and decreased response in WT mice injected with the NKT cell-activating ligand αGalCer. Our finding that NKT cells reduce IgE production by B cells is in line with studies of IgE responses to the model antigen ovalbumin (49, 50). On the other hand, NKT cells have also been shown to provide B-cell help in both T-cell–dependent and T-cell–independent antibody responses (51, 52). Interestingly, a recent report demonstrated that activated NKT cells inhibit autoreactive B cells but activate nonautoreactive B cells (53).

Our finding that IL-18–induced antibody production is increased in NKT cell-deficient mice is in contrast to a previous report where NKT cells were shown to be needed for IL-18–induced IgE production (10). However, in the previous study, $CD1d1^{-/-}$ mice were used to test the IL-18 response in the absence of NKT cells and we show here that these mice lack MZB cells when they are not fully backcrossed. Differences in the MZB population between the different NKT cell-deficient mice used could thus explain the discrepancy in the results. This notion is further supported by the fact that we found MZBs to be an important component of IL-18–induced antibody production, as illustrated by the delayed antibody response in MZB-deficient ($CD19^{-/-}$) mice.

The increased antibody response in NKT cell-deficient mice was accompanied by a shift to a more mature GC reaction compared with that in WT mice as illustrated by an increase in *aid* and a decrease in *ebi2* expression. These results show that NKT cells balance the innate antibody response induced by an inflammatory cytokine by limiting the humoral response. Mechanistically, we find evidence for involvement of both the perforin and the CD95/CD178 pathways. It has been reported that NKT cells kill CD1d-expressing targets, especially MZBs, loaded with αGalCer and that this process preferably involves the CD95/CD178 pathway (16). Our data suggest that in response to innate autoinflammatory responses induced by IL-18, NKT cells use several cytotoxicity pathways to control the self-reactive B-cell activation. Thus, NKT cells may regulate the magnitude of the response to several innate inflammatory signals, and one can envision that this process also may translate to memory responses.

In summary, we have described a unique mechanism by which a product of inflammasome activation leads to induced production of innate antibodies. Moreover, we demonstrate that the presence of NKT cells prevents inherently autoreactive B cells from entering a GC reaction. We suggest that induction of the inherited antibody repertoire is beneficial to protect from invading pathogens but strictly controlled by NKT cells to avoid production of pathogenic antibodies that can add to autoimmunity and IgE-mediated diseases. Taken together, these find-

ings give insights into how inflammatory responses are kept in check and describe potential targets for regulation of inflammatory diseases.

Materials and Methods

Mice. 129S6/SvEvTac (129/SvEv) mice were from Taconic and CD19$^{-/-}$ mice (54) on a 129/SvEv background were kindly provided by Nils Lycke (Gothenburg University, Gothenburg, Sweden). Mice deficient in CD4 (20), IFNγR (35), and perforin (55) were all on the C57BL/6 background. CD1d$^{-/-}$ mice (56) and Jα18$^{-/-}$ mice (57) on the C57BL/6 background (backcrossed for >10 generations) as well as CD1d1$^{-/-}$ mice (33) backcrossed to the C57BL/6 strain for 6 generations were kindly provided by Maria Johansson and Petter Höglund (Karolinska Institute). CD1d1$^{-/-}$ mice (33) backcrossed to the C57BL/6 strain for >10 generations were kindly provided by Michiko Shimoda (Georgia's Health Sciences University). Mice deficient in CD178/FasL (no. 001021) and C57BL/6J controls (000664) were purchased from The Jackson Laboratory. Animals were kept and bred under pathogen-free conditions at the animal facility of the Department of Microbiology, Tumor and Cell Biology, Karolinska Institute. The experiments were approved by the local ethical committee (North Stockholm district court).

Injections. Age- and sex-matched 8- to 10-wk-old mice were injected with 2 μg rmIL-18 (MBL) or PBS i.p. daily for 2–10 d. The serum antibody levels were monitored throughout the experiment, and spleens and/or peritoneal lavage were collected on days 2, 4, 6, 8, 10, 12, and 14. The rmIL-18 contained <0.005 ng/mL LPS as measured by the Limulus Amebocyte Lysate endochrome method (Endosafe; Charles River). When αGalCer was combined with IL-18, mice also received 5 μg αGalCer (KRN7000; Diagnocine) i.p. on days 0, 3, 6, and 9. Ten-week-old CD19$^{-/-}$ mice were injected with 10 μg rhBAFF (Peprotech) i.v. three times (days 0, 2, and 4) and the spleen was analyzed for MZBs on day 6. For the spontaneous IgE production experiment, serum samples were collected over time, starting at 6 wk of age.

BM Transfer. Lethally irradiated (900 rad) CD1d1$^{-/-}$ recipient mice were injected i.v. with 2.5×10^6 CD1d$^{-/-}$-derived BM cells. Ten weeks after BM transfer the mice were injected with IL-18 daily for 10 d or left untreated until killed on day 12.

ELISA. Antibodies in sera and cell culture supernatants were measured by standard ELISA techniques. Total IgM and IgG were captured with purified anti-mouse IgH+L (Southern Biotech) and total IgE with purified anti-mouse IgE (BD Pharmingen). Specific antibodies against PC, NP, and DNA were captured with PC-BSA (a kind gift from Athera Biotechnologies), NP_{26}-BSA (Biosearch Technologies), and methylated BSA plus calf thymus DNA (Sigma-Aldrich), as described previously (18). All antibodies were detected with AP-conjugated secondary anti-mouse IgM, IgG, IgG_1, IgG_{2a}, IgG_{2b}, IgG_3, and IgE (Southern Biotech). Mouse control IgG (ProSci) as well as purified isotype controls for mouse IgM, IgE (BD Pharmingen), IgG_1, IgG_{2a}, IgG_{2b}, and IgG_3 (BioLegend) served as standards. BAFF in sera was measured by a specific ELISA kit (Alexis) according to the manufacturer's instructions. All samples were tested in duplicate.

Affinity Determination. Biosensors have been shown to measure antibody affinity with high sensitivity (58), and the binding kinetics of the anti-NP antibodies in sera of IL-18–injected mice were determined using an Attana 100 Quartz Crystal Microbalance. NP_4-BSA was immobilized on an LNB Carboxyl-Chip (Attana) by amine coupling according to the manufacturer's instructions. Pooled sera from preimmune (PI) or IL-18–injected WT (C57BL/6) or CD1d$^{-/-}$ mice were diluted 1:20 and flowed over the chip. The data were sampled and analyzed using Attester and Evaluation software, respectively (Attana).

Cell Culture and β-Hexosaminidase Release Assay. Mouse BM was differentiated into mast cells (BMMCs) by culture in media supplemented with IL-3, as described previously (59). The BMMCs were then incubated for 90 min with 10% sera from IL-18–injected mice followed by cross-linking for 30 min with 2 μg/mL purified anti-mouse IgE (R35-72; BD Pharmingen). The granular enzyme β-hexosaminidase was analyzed in the BMMC supernatant as a measure of degranulation, as described previously (59).

For ex vivo cell cultures, spleen and peritoneal lavage were collected from untreated and IL-18–injected mice. The spleens were strained through a 100-μm nylon mesh and erythrocytes in the single-cell suspension were lysed with ACK buffer (0.15 M NH_4Cl, 1 mM $KHCO_3$, 0.1 mM EDTA, pH 7.2). The splenocytes and peritoneal cells were cultured in RPMI-1640 media (HyClone), supplemented with 10% heat-inactivated FCS (Invitrogen), 2 mM L-glutamine, 100 units/mL penicillin, 100 μg/mL streptomycin, and 5 μM mercaptoethanol (Sigma-Aldrich) at 37 °C with 5% CO_2. For antibody production, supernatants were collected after 6 d of culture. For assessment of cytokine production, splenocytes were stimulated with LPS (10 μg/mL; Sigma) or anti-CD3 (3 μg/mL, clone 145–2C11; BD Pharmingen) for 48 h after which supernatants were analyzed with the CBA Mouse Th1/Th2/Th17 kit according to the manufacturer's instructions (BD Pharmingen).

Flow Cytometry. Splenocytes in single-cell suspension were first blocked with purified anti-mouse CD16/32 (Fc-block; BD Pharmingen) to reduce unspecific labeling and the cells were thereafter stained with anti-mouse antibodies binding CD5 (clone 53-7.3), CD19 (1D3), CD21/35 (7G6), CD23 (B3B4), CD95 (Jo2), CD138 (281-2), GL7 and TCR-β (H57-597) (BD Pharmingen), CD93 (AA4.1; eBioscience), IL-18Rα (RnD Systems), B220 (RA3-6B2), IgM (RMM-1), and fluorescently labeled streptavidin (BioLegend). NKT cells were detected using CD1d-dimerX loaded with αGalCer (KRN7000; Larodan Fine Chemicals) as suggested by the manufacturer (BD Pharmingen) and fluorescently labeled using a polyclonal anti-mouse IgG_1 antibody conjugated with a488 or a647 (Invitrogen). For intracellular staining of IgE (R35-72) and IgG_1 (A85-1; BD Pharmingen), the cells were treated with fixation buffer and permeabilization wash buffer (BioLegend) according to the manufacturer's instructions and dead cells were excluded using the LIVE/DEAD fixable dead cell strain kit (Invitrogen). Samples were analyzed on a FACSCalibur or FACSAria (Becton Dickinson), using FlowJo software (Tree Star). A minimum of 150,000 events were collected for each sample.

Histology. Spleens were frozen in OCT (Sakuru) and cut in 8-μm thin sections in a cryostat microtome. The sections were dried overnight, fixed in acetone, and blocked with 5% goat sera (Dako) and an avidin/biotin blocking kit (Vector Laboratories) before staining with the following anti-mouse antibodies: B220-FITC and allophycocyanin, CD1d-biotin (1B1), CD4-FITC (RM4-5, pseudocolored blue), CD138-biotin, IgG_1-FITC, IgE-biotin (R35-118) (BD Pharmingen), F4/80-allophycocyanin (BM8; eBioscience), IL-18 Rα-biotin (RnD Systems), PNA-biotin (Vector Laboratories), and streptavidin-Qdot605 or streptavidin-a555 (Invitrogen). Images were collected using a confocal laser scanning microscope (Leica TCS SP2) equipped with one argon and two HeNe lasers and processed in Photoshop software (Adobe Systems).

Quantitative RT-PCR. Total RNA was extracted from mouse spleens by the TRIzol method (Invitrogen) and a reverse transcriptase reaction was performed using the iScript cDNA synthesis kit (Bio-Rad). Quantitative RT-PCR was conducted with Rotor-Gene Q (Qiagen), using IQ SYBR Green Supermix (Bio-Rad) and specific primer pairs for *aid* (5′-AACCCAATTTTCAGATCGCG-3′, 5′-AGCGGTTCCTGGCTATGATAAC-3′), *ebi2/gpr183* (5′-CAGCTTTACCCACTCGGATA-3′, 5′-AAGAAGCGGTCTATGCTCAA-3′), *gapdh* (5′-TGAAGCAGGCATCTGAGGG-3′, 5′-CGAAGGTGGAAGAGTGGGAG-3′), *ifnγ* (5′-CATTGAAAGCCTAGAAAGTCTGAATAAC-3′, 5′-ATCCTTTTTCGCCTTGCTGTTGC-3′), *il4* (5′-GGTCTCAACCCCCAGCTAGT-3', 5′-GCCGATGATCTCTCTCAAGTGAT-3′), *il10* (5′-GGACTGCCTTCAGCCAGGTGA-3′, 5′-TGGGCCTGCTTCTCTGCCT-3′), and *il21* (5′-GGACCCTTGTCTGTCTGGTAG-3′, 5′-TGTGGAGCTGATAGAAGTTCAGG-3′).

Statistical Analysis. The data were analyzed using a Mann–Whitney *U* test to compare two groups. A P value <0.05 was considered statistically significant.

ACKNOWLEDGMENTS. We thank Fredrik Wermeling, Emma Lindh, Ola Winqvist, Mattias Enoksson, Ola B. Nilsson, Hans Grönlund, Petter Höglund, Klas Kärre, Maria Johansson (Karolinska Institute), Nils Lycke, Susanna Cardell (Gothenburg University), Rodolphe Guinamard (Centre d'Immunologie de Marseille-Luminy), Elizabeth Leadbetter (Tradeu Institute), Agnès Lehuen (Institut National de la Santé et de la Recherche Médicale), and Luc Van Kaer (Vanderbilt University School of Medicine) for reagents and/or helpful discussions. This study was supported by grants from the Swedish Research Council, the Center for Allergy Research of Karolinska Institute, the Swedish Medical Society, the Lupus Research Institute, the National Institutes of Health (Grant AI092213 to T.L.M.), King Gustaf V's 80-Year Foundation, and the Magnus Bergvall Foundation. S.L.E. and E.K.G. are supported by a PhD fellowship from Karolinska Institute.

1. Nakanishi K, Yoshimoto T, Tsutsui H, Okamura H (2001) Interleukin-18 regulates both Th1 and Th2 responses. *Annu Rev Immunol* 19:423–474.

2. Sims JE, Smith DE (2010) The IL-1 family: Regulators of immunity. *Nat Rev Immunol* 10: 89–102.

3. Hoshino T, Yagita H, Ortaldo JR, Wiltrout RH, Young HA (2000) In vivo administration of IL-18 can induce IgE production through Th2 cytokine induction and up-regulation of CD40 ligand (CD154) expression on CD4+ T cells. *Eur J Immunol* 30: 1998–2006.
4. Yoshimoto T, et al. (1999) IL-18, although antiallergic when administered with IL-12, stimulates IL-4 and histamine release by basophils. *Proc Natl Acad Sci USA* 96: 13962–13966.
5. Yoshimoto T, et al. (2000) IL-18 induction of IgE: Dependence on CD4+ T cells, IL-4 and STAT6. *Nat Immunol* 1:132–137.
6. Tanaka T, et al. (2001) Interleukin-18 is elevated in the sera from patients with atopic dermatitis and from atopic dermatitis model mice, NC/Nga. *Int Arch Allergy Immunol* 125:236–240.
7. Konishi H, et al. (2002) IL-18 contributes to the spontaneous development of atopic dermatitis-like inflammatory skin lesion independently of IgE/stat6 under specific pathogen-free conditions. *Proc Natl Acad Sci USA* 99:11340–11345.
8. Lind SM, et al. (2009) IL-18 skews the invariant NKT-cell population via autoreactive activation in atopic eczema. *Eur J Immunol* 39:2293–2301.
9. Boraschi D, Dinarello CA (2006) IL-18 in autoimmunity: Review. *Eur Cytokine Netw* 17: 224–252.
10. Yoshimoto T, et al. (2003) Nonredundant roles for CD1d-restricted natural killer T cells and conventional CD4+ T cells in the induction of immunoglobulin E antibodies in response to interleukin 18 treatment of mice. *J Exp Med* 197:997–1005.
11. Viau M, Zouali M (2005) B-lymphocytes, innate immunity, and autoimmunity. *Clin Immunol* 114:17–26.
12. Bendelac A, Bonneville M, Kearney JF (2001) Autoreactivity by design: Innate B and T lymphocytes. *Nat Rev Immunol* 1:177–186.
13. Kearney JF (2005) Innate-like B cells. *Springer Semin Immunopathol* 26:377–383.
14. Wardemann H, et al. (2003) Predominant autoantibody production by early human B cell precursors. *Science* 301:1374–1377.
15. Lang GA, Devera TS, Lang ML (2008) Requirement for CD1d expression by B cells to stimulate NKT cell-enhanced antibody production. *Blood* 111:2158–2162.
16. Wingender G, Krebs P, Beutler B, Kronenberg M (2010) Antigen-specific cytotoxicity by invariant NKT cells in vivo is CD95/CD178-dependent and is correlated with antigenic potency. *J Immunol* 185:2721–2729.
17. Wu L, Van Kaer L (2009) Natural killer T cells and autoimmune disease. *Curr Mol Med* 9:4–14.
18. Wermeling F, Lind SM, Jordö ED, Cardell SL, Karlsson MC (2010) Invariant NKT cells limit activation of autoreactive CD1d-positive B cells. *J Exp Med* 207:943–952.
19. Debets R, et al. (2000) IL-18 receptors, their role in ligand binding and function: Anti-IL-1RAcPL antibody, a potent antagonist of IL-18. *J Immunol* 165:4950–4956.
20. Rahemtulla A, et al. (1991) Normal development and function of CD8+ cells but markedly decreased helper cell activity in mice lacking CD4. *Nature* 353:180–184.
21. Mackay F, et al. (1999) Mice transgenic for BAFF develop lymphocytic disorders along with autoimmune manifestations. *J Exp Med* 190:1697–1710.
22. Evans JG, et al. (2007) Novel suppressive function of transitional 2 B cells in experimental arthritis. *J Immunol* 178:7868–7878.
23. Makowska A, Faizunnessa NN, Anderson P, Midtvedt T, Cardell S (1999) CD1high B cells: A population of mixed origin. *Eur J Immunol* 29:3285–3294.
24. MacLennan IC, et al. (2003) Extrafollicular antibody responses. *Immunol Rev* 194:8–18.
25. Balázs M, Martin F, Zhou T, Kearney J (2002) Blood dendritic cells interact with splenic marginal zone B cells to initiate T-independent immune responses. *Immunity* 17: 341–352.
26. Chan TD, et al. (2009) Antigen affinity controls rapid T-dependent antibody production by driving the expansion rather than the differentiation or extrafollicular migration of early plasmablasts. *J Immunol* 183:3139–3149.
27. Sanderson RD, Lalor P, Bernfield M (1989) B lymphocytes express and lose syndecan at specific stages of differentiation. *Cell Regul* 1:27–35.
28. Honjo T, Kinoshita K, Muramatsu M (2002) Molecular mechanism of class switch recombination: Linkage with somatic hypermutation. *Annu Rev Immunol* 20:165–196.
29. Shaffer AL, et al. (2000) BCL-6 represses genes that function in lymphocyte differentiation, inflammation, and cell cycle control. *Immunity* 13:199–212.
30. Gatto D, Paus D, Basten A, Mackay CR, Brink R (2009) Guidance of B cells by the orphan G protein-coupled receptor EBI2 shapes humoral immune responses. *Immunity* 31:259–269.
31. Pereira JP, Kelly LM, Xu Y, Cyster JG (2009) EBI2 mediates B cell segregation between the outer and centre follicle. *Nature* 460:1122–1126.
32. El Shikh ME, El Sayed RM, Szakal AK, Tew JG (2009) T-independent antibody responses to T-dependent antigens: A novel follicular dendritic cell-dependent activity. *J Immunol* 182:3482–3491.
33. Mendiratta SK, et al. (1997) CD1d1 mutant mice are deficient in natural T cells that promptly produce IL-4. *Immunity* 6:469–477.
34. McCoy KD, et al. (2006) Natural IgE production in the absence of MHC class II cognate help. *Immunity* 24:329–339.
35. Huang S, et al. (1993) Immune response in mice that lack the interferon-gamma receptor. *Science* 259:1742–1745.
36. Coquet JM, et al. (2007) IL-21 is produced by NKT cells and modulates NKT cell activation and cytokine production. *J Immunol* 178:2827–2834.
37. Ozaki K, et al. (2004) Regulation of B cell differentiation and plasma cell generation by IL-21, a novel inducer of Blimp-1 and Bcl-6. *J Immunol* 173:5361–5371.
38. Russell JH, Ley TJ (2002) Lymphocyte-mediated cytotoxicity. *Annu Rev Immunol* 20: 323–370.
39. Li HF, Nookala S, Re F (2007) Aluminum hydroxide adjuvants activate caspase-1 and induce IL-1beta and IL-18 release. *J Immunol* 178:5271–5276.
40. Eisenbarth SC, Colegio OR, O'Connor W, Sutterwala FS, Flavell RA (2008) Crucial role for the Nalp3 inflammasome in the immunostimulatory properties of aluminium adjuvants. *Nature* 453:1122–1126.
41. Bothwell ALM, et al. (1981) Heavy chain variable region contribution to the NPb family of antibodies: Somatic mutation evident in a gamma 2a variable region. *Cell* 24:625–637.
42. Berek C, Berger A, Apel M (1991) Maturation of the immune response in germinal centers. *Cell* 67:1121–1129.
43. Paus D, et al. (2006) Antigen recognition strength regulates the choice between extrafollicular plasma cell and germinal center B cell differentiation. *J Exp Med* 203: 1081–1091.
44. Shlomchik MJ (2008) Sites and stages of autoreactive B cell activation and regulation. *Immunity* 28:18–28.
45. Kang JS, et al. (2006) B cell-activating factor is a novel diagnosis parameter for asthma. *Int Arch Allergy Immunol* 141:181–188.
46. Mackay F, Silveira PA, Brink R (2007) B cells and the BAFF/APRIL axis: Fast-forward on autoimmunity and signaling. *Curr Opin Immunol* 19:327–336.
47. Jacobson BA, et al. (1995) Anatomy of autoantibody production: Dominant localization of antibody-producing cells to T cell zones in Fas-deficient mice. *Immunity* 3:509–519.
48. Wang DN, Wells SM, Stall AM, Kabat EA (1994) Reaction of germinal centers in the T-cell-independent response to the bacterial polysaccharide alpha(1—>6)dextran. *Proc Natl Acad Sci USA* 91:2502–2506.
49. Cui J, et al. (1999) Inhibition of T helper cell type 2 cell differentiation and immunoglobulin E response by ligand-activated Valpha14 natural killer T cells. *J Exp Med* 190:783–792.
50. Harada M, et al. (2006) IL-21-induced Bepsilon cell apoptosis mediated by natural killer T cells suppresses IgE responses. *J Exp Med* 203:2929–2937.
51. Leadbetter EA, et al. (2008) NK T cells provide lipid antigen-specific cognate help for B cells. *Proc Natl Acad Sci USA* 105:8339–8344.
52. Lang GA, Exley MA, Lang ML (2006) The CD1d-binding glycolipid alpha-galactosylceramide enhances humoral immunity to T-dependent and T-independent antigen in a CD1d-dependent manner. *Immunology* 119:116–125.
53. Yang JQ, Wen XS, Kim PJ, Singh RR (2011) Invariant NKT cells inhibit autoreactive B cells in a contact- and CD1d-dependent manner. *J Immunol* 186:1512–1520.
54. Rickert RC, Rajewsky K, Roes J (1995) Impairment of T-cell-dependent B-cell responses and B-1 cell development in CD19-deficient mice. *Nature* 376:352–355.
55. Kägi D, et al. (1994) Cytotoxicity mediated by T cells and natural killer cells is greatly impaired in perforin-deficient mice. *Nature* 369:31–37.
56. Chen YH, Chiu NM, Mandal M, Wang N, Wang CR (1997) Impaired NK1+ T cell development and early IL-4 production in CD1-deficient mice. *Immunity* 6:459–467.
57. Cui J, et al. (1997) Requirement for Valpha14 NKT cells in IL-12-mediated rejection of tumors. *Science* 278:1623–1626.
58. Douagi I, et al. (2010) Influence of novel CD4 binding-defective HIV-1 envelope glycoprotein immunogens on neutralizing antibody and T-cell responses in nonhuman primates. *J Virol* 84:1683–1695.
59. Selander C, Engblom C, Nilsson G, Scheynius A, Andersson CL (2009) TLR2/MyD88-dependent and -independent activation of mast cell IgE responses by the skin commensal yeast Malassezia sympodialis. *J Immunol* 182:4208–4216.